CLM - R 186

CLM - R 186

UKAEA

Report

AN ELECTROSTATIC ANALYSER FOR LASER-PRODUCED PLASMAS: ION SPECTRA FOR POLYTHENE AT 10.6 μm

M W McGEOCH

CULHAM LABORATORY
Abingdon Oxfordshire

1978

Available from H. M. Stationery Office

C/18

£1.00

CLM-R 186

AN ELECTROSTATIC ANALYSER FOR LASER-PRODUCED PLASMAS: ION SPECTRA FOR POLYTHENE AT 10.6 μm

M.W. McGeoch

Culham Laboratory, Abingdon, Oxon., OX14 3DB, UK.
(Euratom/UKAEA Fusion Association)

A B S T R A C T

The design is described of an electrostatic ion energy analyser suitable for the energy range 500 eV to 30 keV/ unit charge. Its use is reported for ~ 1 kJ, 10.6 μm laser pulses incident on plane polythene targets and isolated polythene pellets. A 'fast' ion component is discerned whose angular dependence suggests an origin in ion turbulent motion rather than electrostatic acceleration.

....

April 1978

SBN 85311 068 9

INTRODUCTION

As a preliminary to the irradiation of D_2 pellets for the production of large, warm plasmas, polythene pellets have been used for modelling purposes in the Culham program on laser heated plasmas.[1] In order for ions to be trapped in the CLEO stellarator the ion energy/charge ($\mathcal{E}/Z$) ratio should not greatly exceed 1 keV/proton charge. Since there had been several reports[2,3,4] of a 'fast' ion component in laser produced plasmas, it was thought necessary to examine the ion spectrum in detail in the conditions of the Culham experiment in order to find the upper permissible limit on laser intensity for the plasma to consist mostly of slower ions. The electrostatic analyser was selected for this job because it could easily be calibrated and with several channels it could record the energy spectrum of every carbon species in a single shot. The maximum design energy/charge ratio was 30 keV/proton charge.

DESIGN AND PERFORMANCE OF THE ANALYSER

The analyser is of standard design.[5] Details of its construction are shown in Fig.1. The slits $S_2 \ldots S_7$ are 3 mm wide giving a resolution $\Delta(\mathcal{E}/Z)/(\mathcal{E}/Z)$ which ranges between 0.15 and 0.04 in going from the channels of lowest to highest $\mathcal{E}/Z$. Slits $S_3 \ldots S_7$ are 20 mm in length, but the entrance slit S_2 is only 10 mm long. This allows a degree of space charge expansion out of the plane of the ion parabolic trajectory without distortion of the relative signal in the channels. Slits $S_3 \ldots S_7$ are respectively at distances x = 2, 4, 8, 12, 16 cm along the analyser baseplate (Fig.1). Since $\mathcal{E}/Z$ is proportional to x the different channels cover a factor of 8 range in $\mathcal{E}/Z$. Attenuation of the plasma entering the spectrometer is achieved by varying slit S_1, which may be set to 0.35 mm, 1.0 mm or 5 mm. The length of S_1 is 15 mm.

Separation of the plasma electrons from ions has been effected at the entrance to the spectrometer either by the use of biased grids $G_1 \ldots G_3$

(Fig.1) or by allowing the plasma to pass through a honeycomb structure crossed by a magnetic field. Identical results have been obtained by each technique for ion energies above 500 eV. However, there was evidence of distortion of the spectrum of lower energy ions due to the 300 gauss magnetic fields used in the separator, so biased grids were employed as a rule and particularly in the work covered by this report. The grids were of 90% transmitting 100 mesh tungsten, G_1 and G_3 being at ground potential, grid G_2 biased to - 50V. The grid separation was 3 mm. Further tungsten meshes M_1 and M_2 (Fig.1) covered the apertures in the analyser plates. The function of M_1 was to remove possible distortions of the electric field near slits $S_2 \ldots S_7$. The analyser top plate was found to be a source of spurious signals which were attributed to slow ions produced following the collision of the most energetic plasma particles with the top plate. A slot was cut along the plate where such particles were striking it and mesh M2 covered the slot to maintain a flat potential surface at that plate.

Charge collection was on flat copper plates at ground potential. In each collector cup a grid biased at - 250V suppressed the emission of secondary electrons. We note that carbon ions of energy 10 keV have a secondary electron emission factor $\gamma = 1.5$,[4] so that suppression of secondaries is hardly necessary in the present experiments. A collector cup in the direct line of flight of plasma particles monitored the total ion current. Coaxial lines carrying the charge signals left the vacuum enclosure through miniature coaxial leadthroughs (Sealectro) and were terminated by the 47Ω input impedance of video amplifiers (TI 72733). These amplifiers were battery supplied and enclosed in a copper box on the side of the spectrometer to minimise electrical interference. The gain of the amplifiers was 180 into the 100Ω line connecting to the oscilloscopes. The amplifier risetime was $\lesssim$ 15 ns, their noise level was < 10 mV and their dynamic range was - 1V → + 2V. Typical oscilloscope data are shown in Fig.4.

The flight tube and spectrometer chamber were evacuated to $< 2\times10^{-5}$ Torr during use in order to avoid distortions of the ion spectrum due to charge exchange with residual oxygen and nitrogen. The general behaviour of charge exchange cross sections is described by Nikolaev et al.[6] The nitrogen ion cross sections may be taken to be indicative of what is to be expected for carbon ions. At all energies the cross section $\sigma_{i,i-1}$ for the transition between charge states i and (i-1) varies strongly with i. In fact, for nitrogen ions in N_2 gas $\sigma_{4,3} = 1\times10^{-15}$ cm^2 and $\sigma_{1,0} = 1\times10^{-16}$ cm^2 at

30 keV/nucleon. Taking a value of 10^{-15} cm^2 in a 100 cm flight tube at $2x10^{-5}$ Torr, 6% loss of ions of a given charge state can occur. The dramatic effect of deliberately introducing gas is shown in Fig.2, in which a broad spectrum of ionic states is reduced to a single species (C^+) by raising the flight tube pressure from $5x10^{-5}$ Torr to $3x10^{-4}$ Torr. It is therefore very important to keep the background gas pressure less than $2x10^{-5}$ Torr, and preferably as low as $5x10^{-6}$ Torr, when using flight distances of about 1m.

The ion current limits imposed by space charge have been discussed by Fleischmann et al[7] for the case of circular entrance and exit apertures. We use the formula given by Goforth[5] for ribbon beams. The deflection ΔZ due to the space charge field must be < 1 cm (≡ half the output slit length). From Ref.5,

$$\Delta Z \simeq \frac{0.8i\ (A/Z)^{\frac{1}{2}}\ (\mathcal{E}/Z)^{\frac{1}{2}}}{\ell E^2}$$

where ℓ is the input slit length in cm, i is the input ion current in mA, A is the atomic mass number of the ions of charge Z, E is the deflecting field in kV/cm and $\mathcal{E}/Z$ is in keV. For example with $\ell = 1.5$ cm, $A/Z = 2$, $\mathcal{E}/Z = 1$ keV and $E = 0.5$ kV/cm we require $i < 0.2$ mA. In our instrument therefore the total ion signal should be $\lesssim 0.02$V to completely avoid space charge effects for ions of energy 1 keV. It was verified by varying slit S_1 that space charge effects were not significant for ion energies as low as 500 eV at signal levels of 0.1V. Typically the current signal observed in the charge collectors behind slits $S_3 \ldots S_7$ was $\lesssim 10^{-4}$A.

When observing plasmas created by kilojoule laser pulses certain precautions had to be taken in the design of the flight tube. So great was the laser energy that significant amounts of adsorbed surface gases were detached from the flight tube walls, raising the flight tube pressure significantly during the passage of the plasma. This was particularly marked when using a simple cylindrical flight tube in the observation of plasmas from plane targets inclined so that laser light could be specularly reflected up the flight tube. The problem was eliminated by the use of conical baffles as shown in Fig.3. It was noted that the number of ions recorded by the analyser decreased by 3 times when the baffles were introduced, although there was no change in the relative ion spectrum. It appears that a degree of plasma guiding can occur in the flight tube which is eliminated when the baffles prevent plasma contact with the tube walls.

REDUCTION OF DATA

Typical analyser data is illustrated in Fig.4. This spectrum corresponds to a laser-plasma of only $\approx$ 50 ns duration, so that the width of individual spikes is a function of instrument velocity resolution. The velocity resolution $\Delta v/v$ follows from the energy resolution $\Delta\mathcal{E}/\mathcal{E}$ which is a function of the slit widths and positions. The duration $\Delta\tau$ of an ion spike from a delta function laser-plasma event also depends on the spike arrival time τ. For our instrument:

Channel =	S_3	S_4	S_5	S_6	S_7
$\Delta\tau$ =	$3\tau/20$	$3\tau/40$	$3\tau/80$	$3\tau/120$	$3\tau/160$

In the analysis of a spectrum, the particle number in the energy range of a given channel is proportional to (height of signal in volts) times $\Delta\tau/Z$.

The ionic species in a given spike is identified by measuring the arrival time and noting that[5]

$$A/Z = \left[\frac{2(\mathcal{E}/Z)}{m_p(R + x/\cos\theta)^2}\right]\tau^2$$

where m_p is the proton mass, R is the distance from the ion source to the input slit, $\theta = 45^\circ$ (for this analyser) and $\mathcal{E}/Z$ is in ergs/proton charge.

The accuracy of the spectrum obtained by these methods is confirmed by the re-synthesised total ion current displayed with the original ion current in Fig.5. The spectrum for this example was similar in complexity to that in Fig.4. A further check on the instrument accuracy is possible using the unambiguous C^+ spectrum of Fig.2(b) and (c). The A/Z values calculated for each channel are equal to 12 within 10% in all cases. In particular, channels S_5, S_6 and S_7 have errors as low as 5%.

ION SPECTRA FROM PLANE POLYTHENE AT VARYING ANGLES OF INCIDENCE

A reference experiment was performed to measure the ion energy spectrum formed by the incidence of approximately 300J, 60 ns, 10.6 μm laser pulses on plane polythene. The geometry of the experiment is shown in Fig.3. The analyser was fixed at 45° to the incident laser beam so that the true angular distribution of ions for normally incident laser light could not be measured. However, the plasma expansion is primarily determined by the direction of the target normal, and the spectrum as a function of φ (Fig.3) can be expected to show the same features as would be seen with the laser incident normally and the analyser angle varying. The laser was believed not to be polarised and polarisation-dependent effects on the ion spectrum[(8)] were not studied.

The laser intensity in the focal spot was estimated from the spot size, the measured pulse energy and pulse temporal structure. It was established by using a diffraction screen to create a number of focal spots of known relative intensity that the full spot diameter at half intensity was ~ 750 μm. Burns on a smooth graphite surface showed a degree of astigmatism in the f/20 focusing optics which implied that the laser intensity varied considerably within the focal spot. The incident pulse was 60 ns FWHM, containing some modulation on a 5 ns timescale, so that the peak intensity could be up to 1.5 times the average intensity. The ion spectra were accurately reproducible from shot to shot, however, the same laser energy and angle of incidence producing precisely the same spectrum on any occasion. Spectra are shown in Figs. 6 and 7 for a laser energy of 270J, which corresponded to an average laser intensity of 1×10^{12} W/cm^2. The hydrogen ion curves have not been plotted because the number of H^+ ions observed was very much less than would be expected from the composition of polythene $(CH_2)_n$. The combination of lower A/Z and lower ion energy lead to stronger space charge effects, so that we believe that the bulk of H^+ ions are not observed because their energy is less than 500 eV.

The interesting features of the data in Figs. 6 and 7 are:

(a) the different charge states have much the same energy in directions nearly normal to the target surface. This is indicative of recombination following the acceleration of a predominantly C^{6+} plasma. The total ion currents (Fig.8) also show a characteristic double hump indicating a degree of recombination;[9]

(b) at angles $\varphi = 30^{o} \rightarrow 50^{o}$ the spectrum appears to consist of two components: an energetic component of charge state $\gtrsim 3$ which is similar to that observed normal to the target, and a lower energy $\lesssim 1$ keV component which is predominantly C^{+}. These components are also observed in the total ion currents of Fig.8. The explanation proposed for this spectrum is best illustrated with reference to Fig.9. The electron temperature must decrease away from the laser axis. While the ionisation state would be 6^{+} on the axis, it would steadily decrease towards the edge of the plasma. Ablation would be in the direction of the continuous arrows. However, if the threshold were to be exceeded for the rapid coupling of electron energy into ion thermal energy, say only in the plasma near the laser axis, then highly charged ions would be ejected into a larger angle than otherwise, giving rise to the dual spectrum at larger angles. The path of these ions is shown by dotted arrows in Fig.9.

Further experiments along the following lines would be interesting:

(a) Investigate spectrum as a function of angle and also laser intensity.

(b) Investigate the polarisation dependence of the turbulent component.

We note that although frequent observation has been made of two ion components[4,10,11] following the irradiation of polythene at 10.6 μm, the actual identity of the species belonging to each component has not previously been ascertained, nor has it been suggested that there may be different spatial origins for the components.

ION SPECTRA FROM POLYTHENE BEADS

Only a few of the laser firings on to $\frac{1}{2}$ mm polythene cubes gave good ion spectrometer data. One reason for this was that polythene work gave way to deuterium work at about the same time as the operation of the spectrometer became fully understood and reliable. The spectrum shown in Fig.10 was from a $\frac{1}{2}$ mm polythene cube irradiated by $\sim$ 1.0 kJ in the same 750 μm spot described previously. The ion pulses in each channel had a duration greater than $\Delta\tau$ which implied that the laser-plasma event was of $\approx$ 1 μs duration. As the laser pulse consisted of an initial $\approx$ 300J, 60 ns spike followed by a 700J, 1 μs 'tail', we infer that the spectrum of Fig.10 corresponded to the sum of the spike and tail ions. The dotted portion of the curves in Fig.10 was inferred from another pellet shot, but could be subject to space charge effects.

It is possible to estimate the ion energy spectrum from a theory(12) of the steady ablation of spherical objects below flux-limited intensities. This applies to the tail of the laser pulse, during which the steady absorbed laser power is $\approx 5 \times 10^8$W. For a $\frac{1}{2}$ mm diameter spherical polythene pellet the theory gives a mean ion energy of 1.6 keV which is somewhat larger than that indicated in Fig.10. However, the mean ion energy scales(12) as $r_p^{-0.7}$, where r_p is the radius of the solid density pellet. The pellet diameter towards the end of the 1 μs tail has increased to $\sim$ 1.5 mm(13) thus explaining the lower energies seen in the experiment. As far as it goes, the experiment lends support to the theory of pellet ablation described in Ref.12. The more energetic particles of higher charge state seen in Fig.10 are associated with the initial laser intensity spike.

CONCLUSIONS

An electrostatic analyser has been designed and built which has proved useful in the study of the large plasmas produced by the incidence of 1 kJ 10.6 μm laser pulses on polythene targets. It has been shown that intensities of $\sim 1 \times 10^{12}$ W/cm^2 produce carbon ions of energy $\sim$ 5 keV, which is becoming too energetic for confinement in the CLEO stellarator. The ion spectra show interesting features which may be attributed to collective processes of electron-ion thermalisation (much discussed in recent literature). Some ion data from polythene pellets is in reasonably good agreement with a recent theory of spherical pellet ablation. The results for polythene may be applied to deuterium, with the appropriate scaling.(12)

REFERENCES

1. WALKER, A.C., McGEOCH, M.W., STAMATAKIS, T., WARD, S., WILLIS, B.L., SPALDING, I.J. - 'Multikilojoule CO_2 Laser Heating of Polythene Pellets' Proc.VIII Eur.Conf.Contr.Fusion and Plasma Physics, Prague (1977)
2. BASOV, N.G. ET AL - Sov.Phys.JETP Lett.18, p.184 (1973)
3. McCALL, G.H. ET AL - Phys.Rev.Lett.30, p.1116 (1973)
4. EHLER, A.W. - J.Appl.Phys.46, p.2464 (1975)
5. GOFORTH, R.R. - Rev.Sci.Instr.47, p.548 (1976)
6. NIKOLAEV, V.S., DMITRIEV, I.S., FATEEVA, L.N., TEPLOVA, Ya.A - Sov. Phys.JETP 13, p.695 (1961)
7. FLEISCHMANN, H.H., ASHBY, D.E.T.F., LARSON, A.V. - Nucl.Fusion 5, p.349 (1965)
8. PEARLMAN, J.S., THOMSON, J.J., MAX, C.E. - Phys.Rev.Lett.38, p.1397 (1977)
9. GOFORTH, R.R., HAMMERLING, P. - J.Appl.Phys.47, p.3918 (1976)
10. STENZ, C., POPOVICS, C., FABRE, E., VIRMONT, J., POQUERUSSE, A., GARBAN, C. - J.Physique 38, p.761 (1977)
11. MARTINEAU, J., PARANTHOEN, P., RABEAU, M., PATOU, C. - Optics Comm.15, p.404 (1975)
12. McGEOCH, M.W. - to be published
13. WALKER, A.C. ET AL - to be published

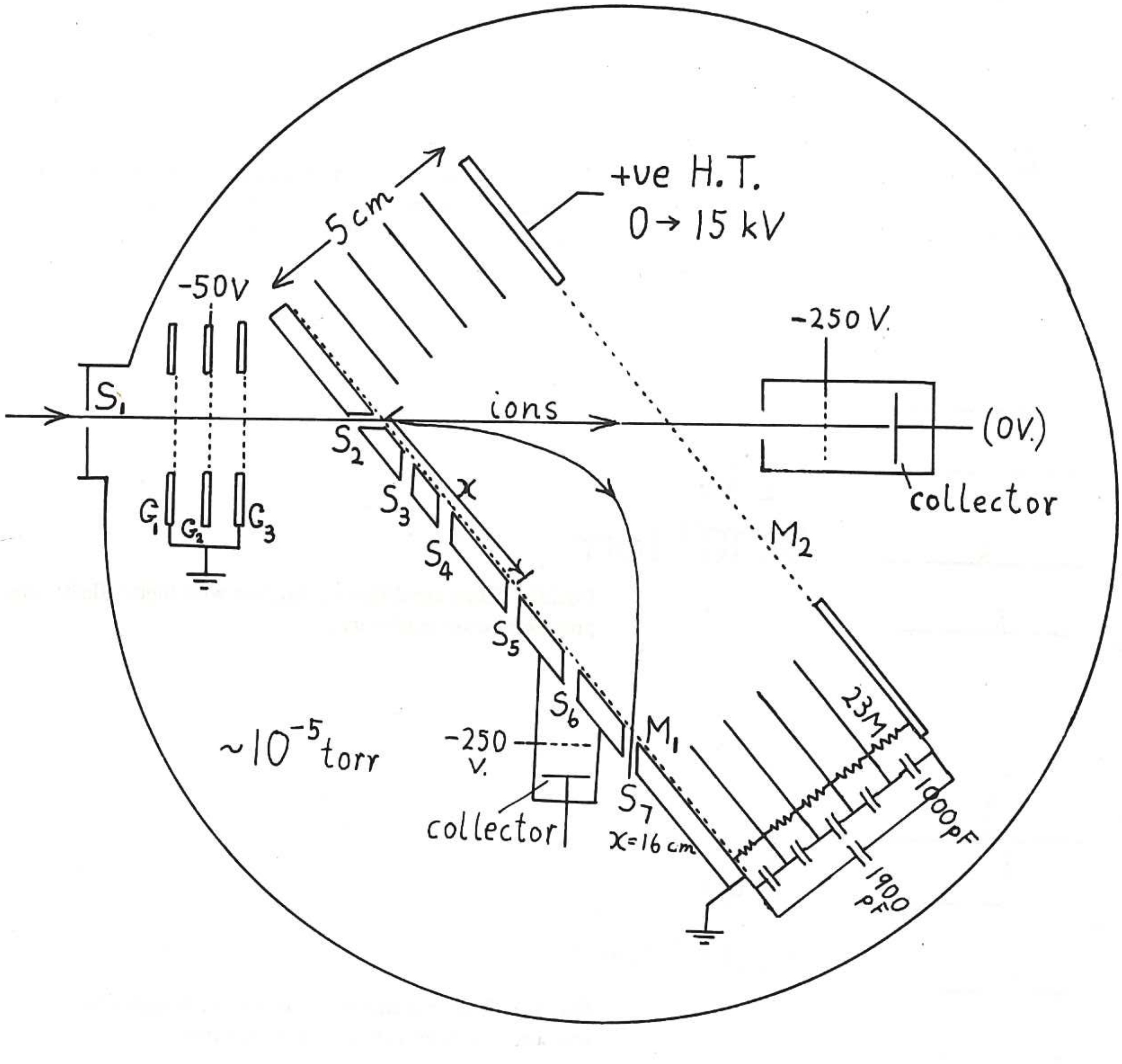

Fig.1 Schematic layout of the analyser.

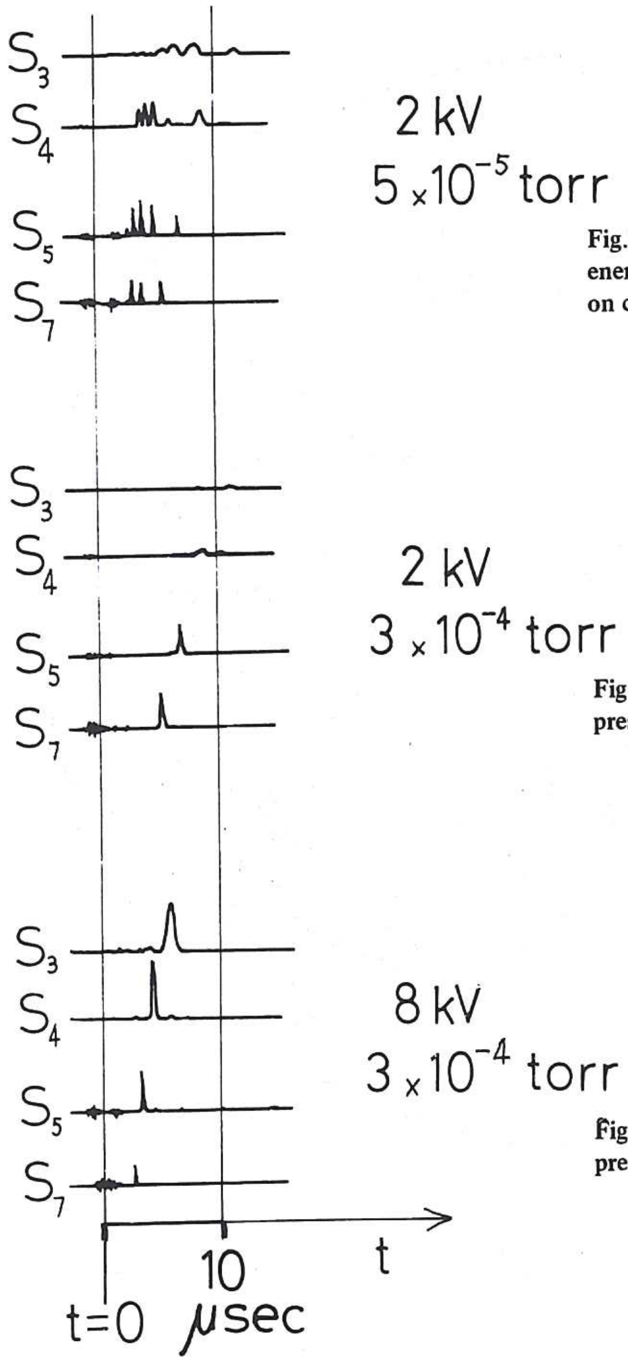

Fig.2(a) Ion spectrum from plane polythene, $\varphi = 40°$, laser energy 270 J in 60 ns. Slit $S_1 = 0.35$ mm and same sensitivity on channels $S_3 \ldots S_7$. Plate voltage 2kV.

Fig.2(b) Same conditions as (a), but with higher flight tube pressure; (same sensitivity).

Fig.2(c) Same conditions as (a), but with higher flight tube pressure and plate voltage; (same sensitivity).

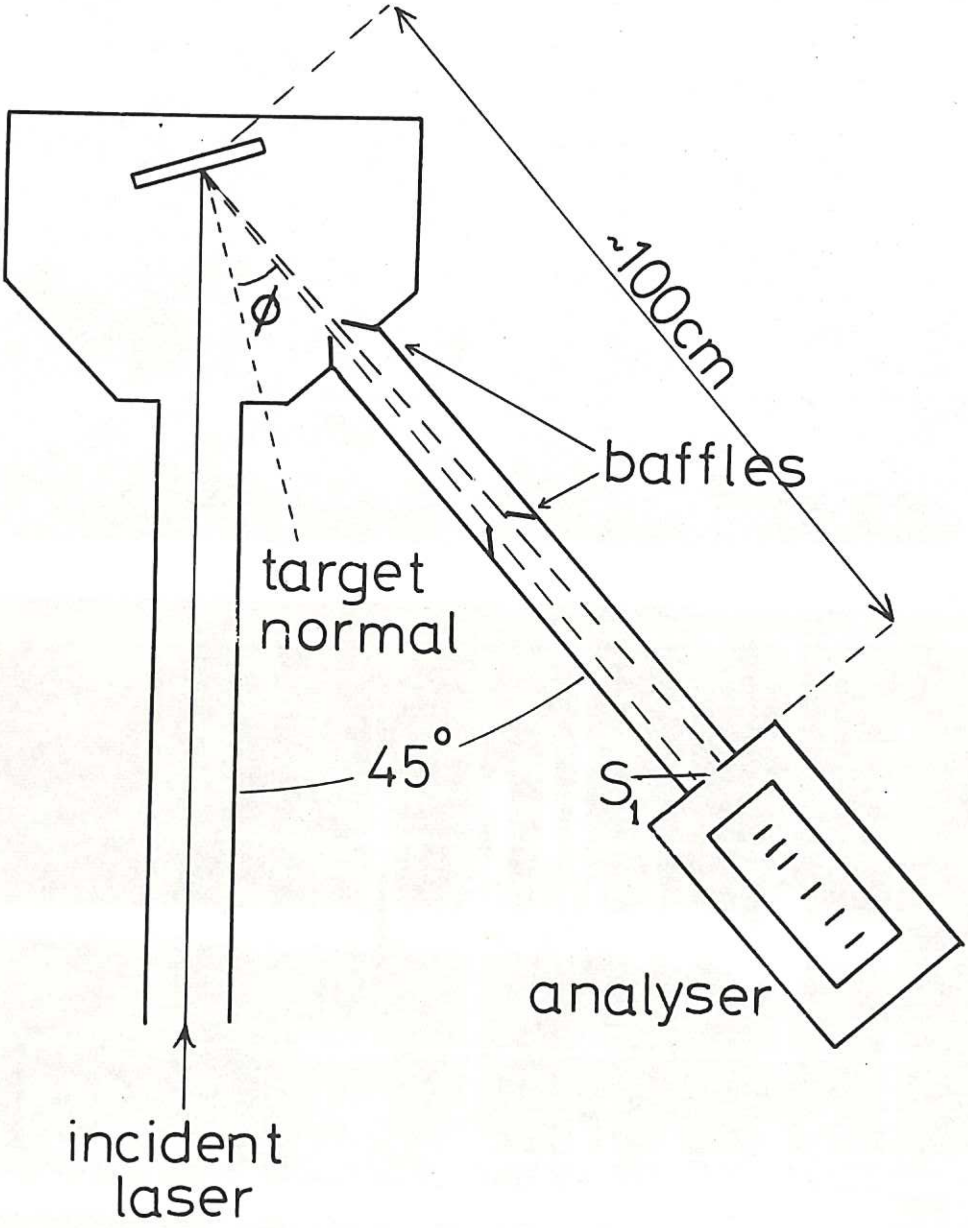

Fig.3 Detail of target disposition and flight tube baffles.

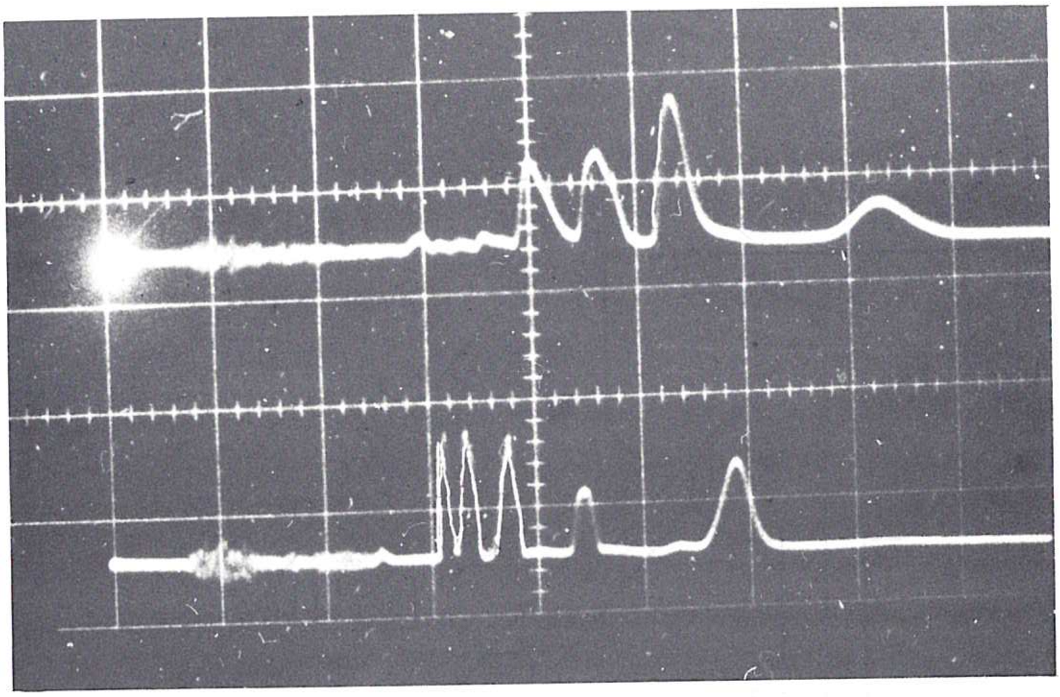

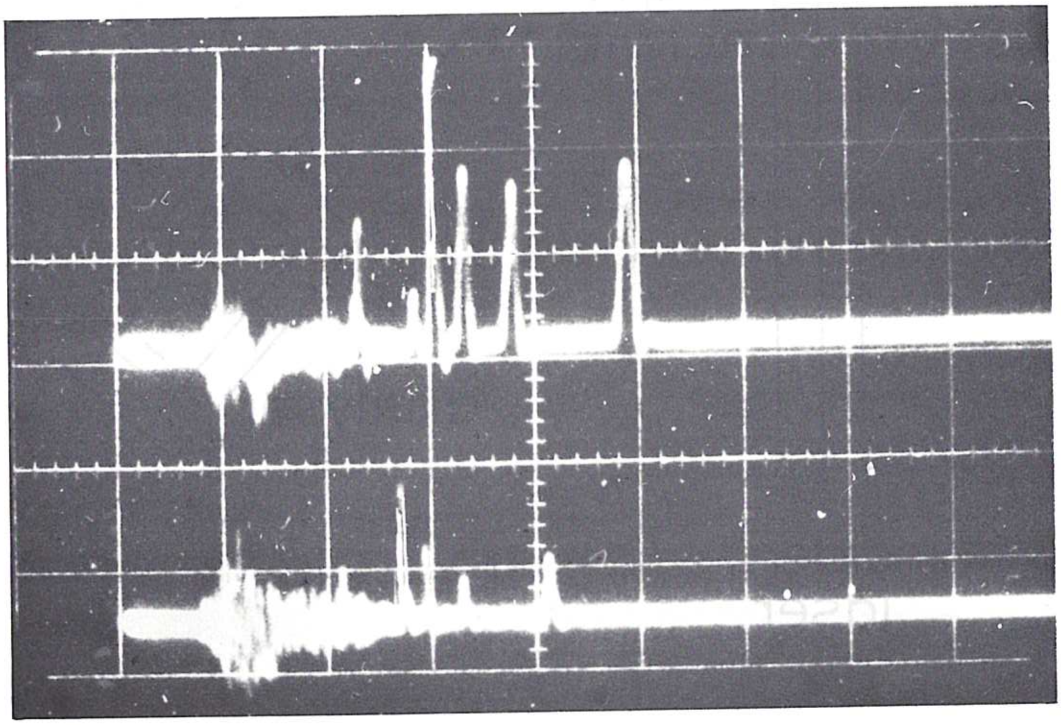

Fig.4 Spectrum from plane polythene, $\varphi = 45°$, slit $S_1 = 0.35$ mm. Traces from slits S_3, S_4, S_5, S_7 are shown (from the top down) all at the same sensitivity. Laser energy 270 J in 60 ns. Timescale 2 μs/div.

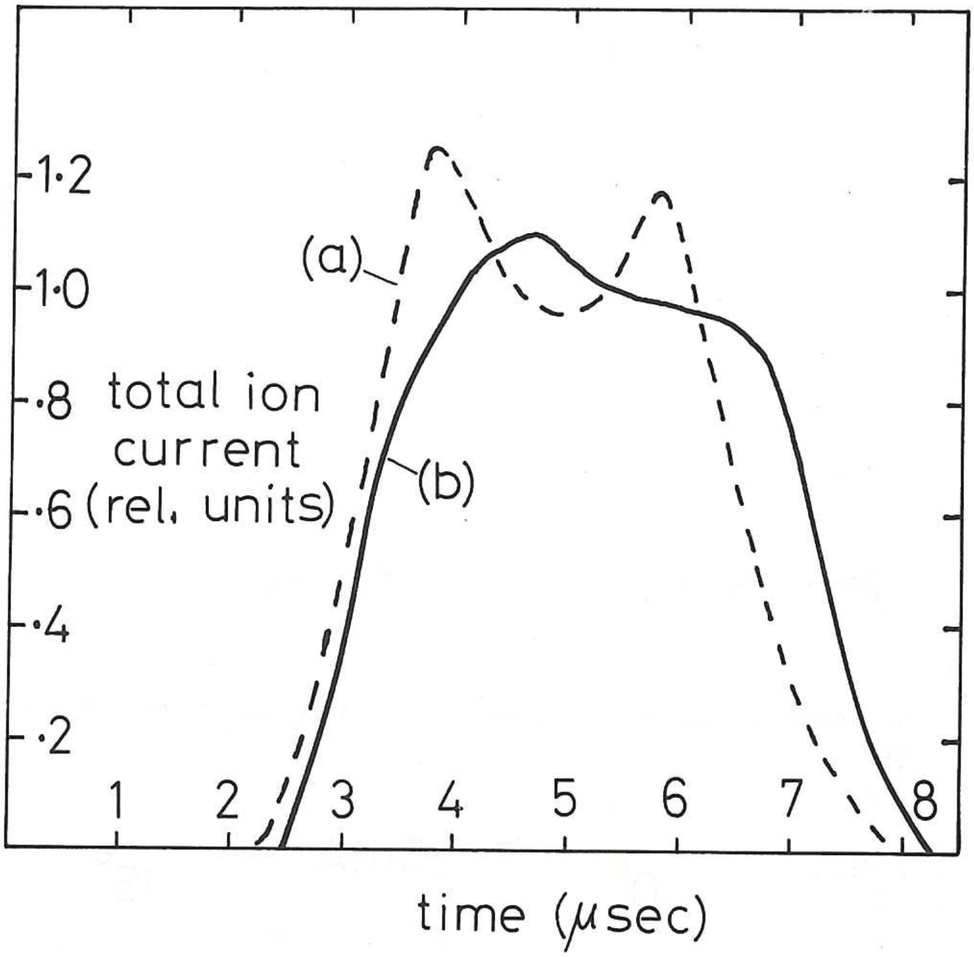

Fig.5 Total ion current at analyser, $\varphi = 15^\circ$, laser energy 270J in 60ns on to plane polythene. Trace (a): direct measurement of ion current. Trace (b): re-synthesised ion current following reduction of spectrum according to text.

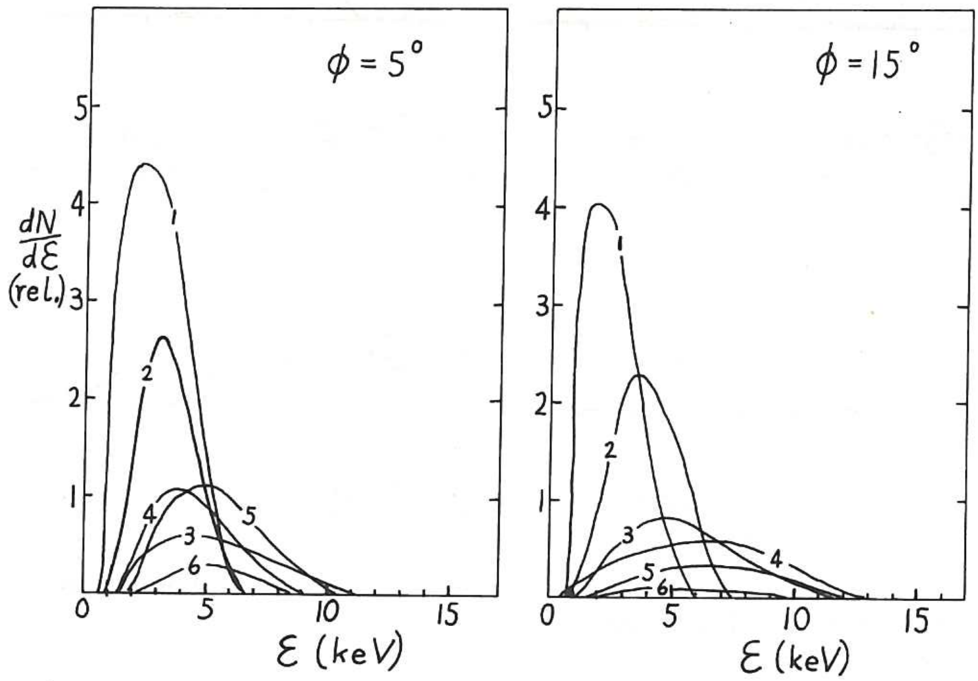

Fig.6 Ion spectra from plane polythene as a function of φ. Laser energy 270J in 60ns. Numbers indicate carbon charge state.

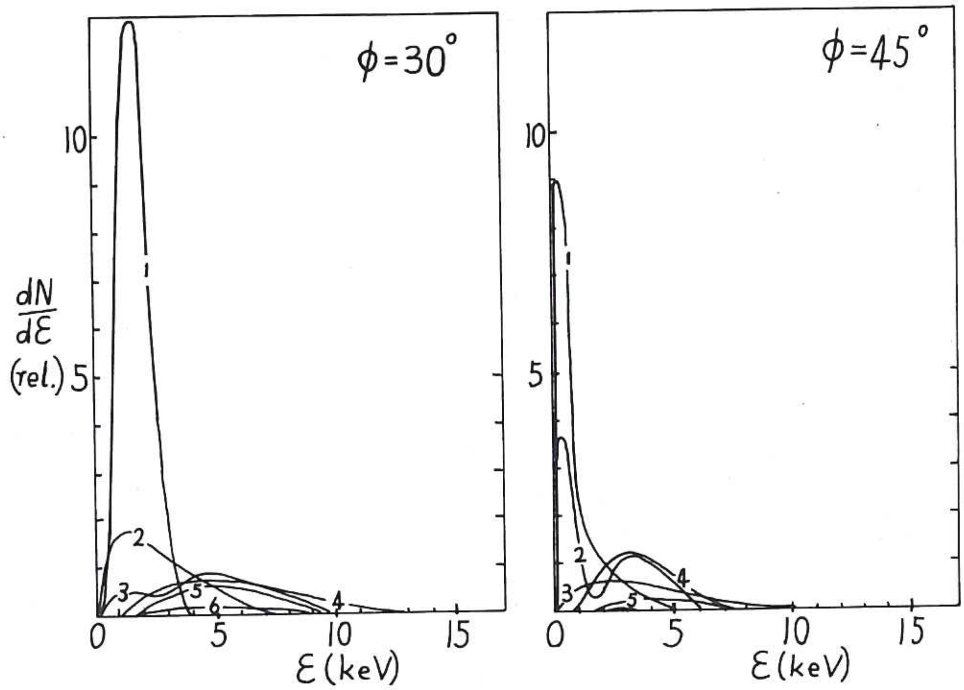

Fig.7 Ion spectra as a function of φ (continued from Fig.6). Same relative scale as in Fig.6.

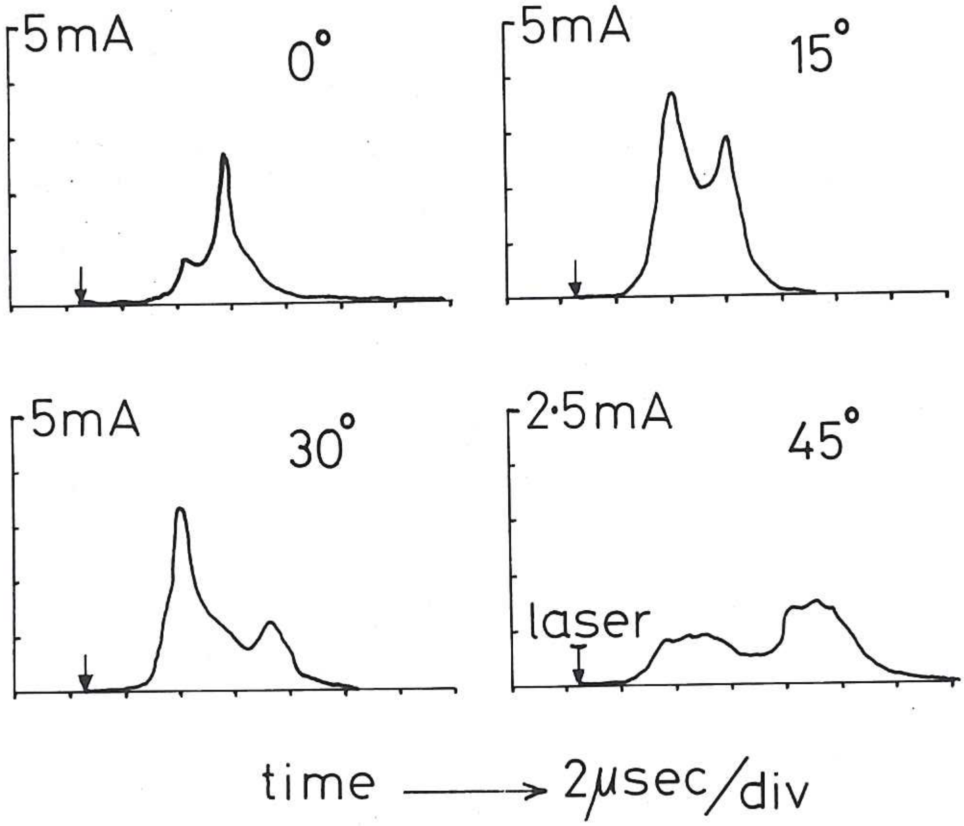

Fig.8 Total ion current at the analyser for various φ. Laser energy 270J in 60ns on to plane polythene. Slit S_1 = 5mm.

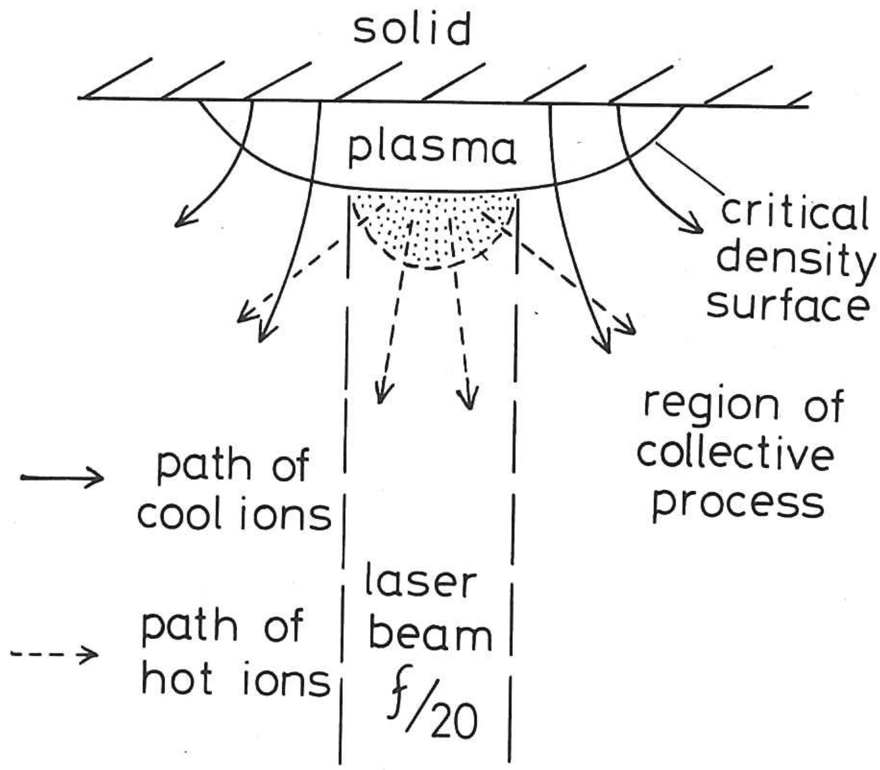

Fig.9 Illustration of possible source for spectral structure as a function of angle.

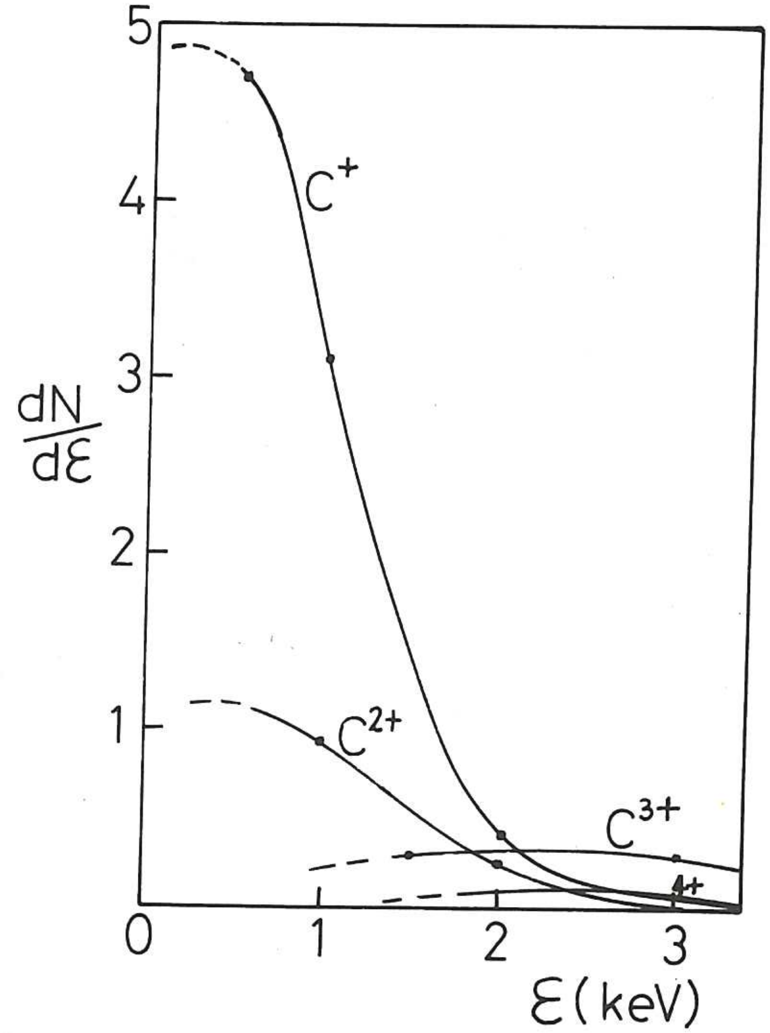

Fig.10 Ion spectrum from ½mm polythene cube irradiated by ~ 1.0 kJ in 1 μs.

HER MAJESTY'S STATIONERY OFFICE

Government Bookshops

49 High Holborn, London WC1V 6HB
13a Castle Street, Edinburgh EH2 3AR
41 The Hayes, Cardiff CF1 1JW
Brazennose Street, Manchester M60 8AS
Wine Street, Bristol BS1 2BQ
258 Broad Street, Birmingham B1 2HE
80 Chichester Street, Belfast BT1 4JY

Government publications are also available through booksellers